Laura K. Cole,[1] Edgard M. Mejia,[1] Marilyne Vandel,[1] Genevieve C. Sparagna,[2] Steven M. Claypool,[3] Laura Dyck-Chan,[1] Julianne Klein,[4] and Grant M. Hatch[1]

Impaired Cardiolipin Biosynthesis Prevents Hepatic Steatosis and Diet-Induced Obesity

Diabetes 2016;65:3289–3300 | DOI: 10.2337/db16-0114

Mitochondria are the nexus of energy metabolism, and consequently their dysfunction has been implicated in the development of metabolic complications and progression to insulin resistance and type 2 diabetes. The unique tetra-acyl phospholipid cardiolipin (CL) is located in the inner mitochondrial membrane, where it maintains mitochondrial integrity. Here we show that knockdown of Tafazzin (TAZ kd), a CL transacylase, in mice results in protection against the development of obesity, insulin resistance, and hepatic steatosis. We determined that hypermetabolism protected TAZ kd mice from weight gain. Unexpectedly, the large reduction of CL in the heart and skeletal muscle of TAZ kd mice was not mirrored in the liver. As a result, TAZ kd mice exhibited normal hepatic mitochondrial supercomplex formation and elevated hepatic fatty acid oxidation. Collectively, these studies identify a key role for hepatic CL remodeling in regulating susceptibility to insulin resistance and as a novel therapeutic target for diet-induced obesity.

Obesity is now a pandemic, with projections of over 1 billion adults worldwide being obese by 2030 (1) and direct costs in excess of $100 billion/year in the U.S. alone (2). Obesity is particularly devastating since excess lipid accumulates in nonadipose tissues, contributing to systemic insulin resistance and elevated risk for the development of type 2 diabetes (3). Progressive mitochondrial dysfunction is associated with lipotoxic-mediated disruption of insulin signaling, including a decline in respiratory chain function, reduced or incomplete fatty acid oxidation (FAO), and overproduction of reactive oxygen species (ROS) (3).

Cardiolipin (CL) regulates numerous mitochondrial proteins and processes as a result of its unique tetra-acyl structure and localization within the inner mitochondrial membrane (4,5). In high metabolic rate tissues, such as heart and skeletal muscle, the predominant form of CL consists of four linoleic acyl side chains (L_4CL) (4,5). Loss of CL and/or L_4CL promotes mitochondrial dysfunction. This is underscored by the development of Barth syndrome (BTHS), a genetic disease characterized by L_4CL deficiency, impaired mitochondrial respiration, dilated cardiomyopathy, and skeletal myopathy (5). Patients with BTHS carry mutations within the Tafazzin (TAZ) gene, which encodes a mitochondrial transacylase required to incorporate linoleic acid into CL (5).

Loss of CL and/or L_4CL has been widely demonstrated in human and animal models of heart failure (4,6–8). One way in which CL content regulates mitochondrial dysfunction is through direct involvement in the assembly and function of respiratory supercomplexes (4). These comprise mainly complex I (NADH–coenzyme Q reductase), complex III (ubiquinol–cytochrome *c* reductase), and complex IV (cytochrome *c* oxidase), and function to promote efficient electron flux to optimize the use of available substrates and control the production of ROS (9). Induced pluripotent stem cells developed from patients with BTHS have decreased supercomplex formation, which coincides with reduced oxygen consumption and increased generation of ROS (10). Indeed, loss of CL content in heart failure is

[1]Children's Hospital Research Institute of Manitoba, Department of Pharmacology & Therapeutics, Faculty of Health Sciences, University of Manitoba, Winnipeg, Canada
[2]Department of Medicine, University of Colorado Denver, Anschutz Medical Campus, Aurora, CO
[3]Department of Physiology, Johns Hopkins University School of Medicine, Baltimore, MD
[4]Diagnostic Services of Manitoba, Winnipeg, Canada
Corresponding author: Grant M. Hatch, ghatch@chrim.ca.

Received 22 January 2016 and accepted 26 July 2016.
This article includes Supplementary Data online at http://diabetes.diabetesjournals.org/lookup/suppl/doi:10.2337/db16-0114/-/DC1.

associated with reduced activity of individual respiratory complexes and impaired mitochondrial respiratory function (6,8).

Despite the role of CL in regulating mitochondrial function, an association with metabolic syndrome has not been examined extensively. The few studies that exist indicate that diet-induced obesity promotes pathological remodeling of CL (11–13). However, it remains unclear whether reduced levels of mitochondrial L_4CL are sufficient to initiate atypical accumulation of lipids in nonadipose tissues and disrupt insulin signaling. We investigated the role of CL and L_4CL levels in the development of diet-induced obesity and insulin resistance with the use of a TAZ knockdown (kd) mouse model (14). Our results establish that TAZ kd prevents the development of hepatic steatosis and obesity that leads to insulin resistance. Furthermore, despite TAZ deficiency, hepatic CL levels were normal and supercomplexes maintained, providing an environment capable of promoting elevated FAO and the hypermetabolism responsible for a lean phenotype.

RESEARCH DESIGN AND METHODS

Animals

This study was performed with the approval of the University of Manitoba Animal Policy and Welfare Committee. All animals were maintained in an environmentally controlled facility (12-h light/12-h dark cycle), with free access to food and water. Experimental animals were generated by mating male transgenic (Tg) mice [B6.Cg-Gt(ROSA)26Sortm1(^{1}H/tetO-RNAi:Taz,CAG-tetR)Bsf/ZkhuJ; The Jackson Laboratory, Bar Harbor, ME], which have a doxycycline (dox)–inducible, TAZ-specific short hairpin RNA (shRNA), with female C57BL/6J mice (The Jackson Laboratory). TAZ kd was induced in utero and maintained postnatally by administering dox (625 mg/kg chow) as part of the standard low-fat (6% fat [w/w]) rodent chow (rodent diet catalog no. TD.01306; Harlan), as described previously (14). Female C57BL/6J mice consumed the dox diet (TD.01306) for at least 4 days before breeding. A low-fat diet lacking dox was used during the 4-day mating period to prevent TAZ kd in the Tg males. Dams were then returned to the dox diet (TD.01306) for their entire pregnancy, birth, and suckling period. Only male offspring were used experimentally; they were weaned at 3 weeks of age onto either the low-fat (6% w/w) (rodent diet catalog no. TD.01306; Harlan) or high-fat (23% w/w) diet (rodent diet catalog no. TD.130261; Harlan) containing dox (625 mg/kg chow). Male mice positive for the TAZ shRNA transgene were identified by PCR using primers (forward: 5′-CCATGGAATTCGAACGCTGACGTC-3′; reverse: 5′-TATGGGCTATGAACTAATGACCC-3′) described elsewhere (14). Nontransgenic (NTg) littermates treated with a dox diet were used as wild-type controls. In addition, some dams and corresponding male offspring (Tg and NTg) were not treated with dox and served as additional experimental controls. Metabolic measurements were obtained using an Omnitech (Columbus, OH) animal monitoring system and expressed per lean body mass. Intestinal absorption was fecal (kilocalories) minus food consumption (kilocalories).

Mitochondrial Analysis

Mitochondrial hydrogen peroxide (H_2O_2) was quantitated using Amplex UltraRed reagent. Mitochondrial supercomplexes (25 μg protein) were separated by Blue Native PAGE, and individual complexes were visualized using in-gel activity assays (4). The oxygen consumption rate (OCR) was measured from mouse hepatocytes (2×10^4/well) and skeletal muscle fibers (10 μg protein/well) isolated from the flexor digitorum brevis using a Seahorse Bioscience instrument. Media contained either 1 mmol/L pyruvate and 25 mmol/L glucose for glucose metabolism or 1 mmol/L pyruvate, 2.5 mmol/L glucose, 0.5 μmol/L carnitine, and 0.175 mmol/L palmitate-BSA for fatty acid (FA) metabolism. Basal oxygen consumption was considered to be the basal respiration sensitive to inhibition by 1 μmol/L antimycin A plus 1 μmol/L rotenone. ATP-sensitive oxygen consumption was inhibited by 1 μmol/L oligomycin, and ATP-insensitive respiration (heat) was the remaining proportion of basal oxygen consumption. Maximal oxygen consumption was achieved with 1 μmol/L carbonyl cyanide 4-(trifluoromethoxy) phenylhydrazone (FCCP) for hepatocytes or 0.4 μmol/L FCCP for skeletal muscle fibers. FA-dependent respiration is the difference in oxygen consumption measured in the presence of 40 μmol/L etomoxir and vehicle (water).

Western Blotting

The mouse monoclonal antibody raised against TAZ (Clone 2G3F7) was affinity purified by Steven Claypool's laboratory at the Johns Hopkins University School of Medicine (15).

Primary Cultures of Hepatocytes

Primary cultures of adult mouse hepatocytes were isolated (16) and treated with serum-free DMEM containing either 2 μCi [^{14}C] oleate plus 0.4 mmol/L oleate-BSA or 2 μCi [^{14}C] acetate per 2-mL dish. Total lipids were extracted (17) and individual species quantitated as previously described (18).

Blood and Tissue Parameters

Plasma levels of tumor necrosis factor-α, insulin, leptin, and adiponectin were quantitated by ELISA (ALPCO). Commercially available kits were used to measure plasma ketones, nonesterified FAs (Wako Diagnostics), and alanine aminotransferase (Biotron Diagnostics Inc.). The mass of triglycerides (TGs), phospholipids, cholesteryl ester, and cholesterol were determined by high-performance liquid chromatography (19) or phosphorus assay (20). Molecular species of CL were quantitated from tissue homogenates by high-performance liquid chromatography coupled to electrospray ionization mass spectrometry (21). Plasma lipoproteins were separated by size using fast-protein liquid chromatography on an Agilent 1200 chromatography system with a Superose 6 column (Amersham Pharmacia Biotech Inc.) and in-line enzymatic assay kits (Thermo Infinity regents) (22). The rate of hepatic TG secretion was measured following a 16-h fast and injection of

Poloxamer 407 (1 g/kg, i.p.) (23). Tissues were fixed in 10% buffered formalin for hematoxylin-eosin (5 μm) staining or 4% paraformaldehyde for Oil Red O (8 μm) staining and scored using a system modified from that used by Kleiner et al. (24).

Statistical Analysis

Data are expressed as means ± SEMs. Comparisons between groups was performed by unpaired, two-tailed Student *t* test or one-way ANOVA using Student-Newman-Keuls post hoc analysis where appropriate. A probability value <0.05 was considered significant.

RESULTS

Hypermetabolism Protects TAZ kd Mice From Obesity, Hepatic Steatosis, Hyperlipidemia, and Insulin Resistance

Male mice Tg for the dox-inducible TAZ shRNA were fed dox to induce TAZ kd. We confirmed a reduction in the TAZ protein in several tissues of the dox-fed Tg animals compared with the NTg dox-fed (Ntg + dox) littermate controls (Fig. 1*A* and Supplementary Fig. 1*A* and *B*).

Over a 10-month period, NTg + dox mice gained excess weight, presumably because of the growth-inducing properties of dietary antibiotics (25) (Fig. 1*B*). By contrast, TAZ kd animals (Tg + dox) had a growth curve that was reduced compared with the littermate controls (NTg + dox) and Tg and NTg mice fed a standard rodent diet (Tg and NTg −dox; Fig. 1*B* and Supplementary Fig. 1*C*). There was no significant difference in bone development between genotypes fed or not fed dox (Supplementary Fig. 1*D* and *E*). We determined that TAZ deficiency significantly reduced adiposity (Fig. 1*C* and *D*), with individual fat pads weighing less (Fig. 1*F* and Supplementary Fig. 1*F* and *G*) and reduced plasma leptin concentrations (~99%; Table 1) compared with littermate controls (NTg + dox). TAZ deficiency limited white adipose tissue (WAT) growth by reducing hypertrophy and hyperplasia and increasing beige cell recruitment (Fig. 1*E* and Supplementary Fig. 1*I–K*). The deleterious accumulation of TGs into the liver and skeletal muscle of NTg + dox mice was also attenuated in TAZ deficiency (Table 1). TAZ kd mice were completely protected from developing hepatic steatosis and had normal histological features (Fig. 1*G* and *J* and Supplementary Fig. 1*H* and *L*) and plasma alanine aminotransferase (ALT) concentrations (Table 1). In aged NTg + dox animals, obesity was accompanied by plasma hyperlipidemia, hyperglycemia, and hyperinsulinemia (Table 1). By contrast, plasma VLDL-TG and LDL-cholesterol concentrations were reduced in TAZ kd animals (Fig. 1*H* and *I*). Furthermore, TAZ deficiency protected against the development of impaired glucose clearance and insulin resistance associated with diet-induced obesity (Fig. 1*K* and *L*).

The decreased body weight of TAZ kd mice could not be accounted for by reduced food consumption, water intake, or intestinal caloric absorption (Fig. 2*A–C*). Alternatively, indirect calorimetry indicated that oxygen consumption (Fig. 2*D* and *H*), heat production (Fig. 2*E* and *I*), and activity (Fig. 2*F* and *J*) were significantly increased in TAZ kd mice compared with NTg + dox littermates. A reduction in the respiratory exchange ratio indicated that the TAZ kd mice were consuming proportionally more fat than carbohydrate during the light cycle (Fig. 2*G* and *K*).

Obesity Is Prevented in TAZ-Deficient Mice Fed a High-Fat Diet

To assess further the protective effect of TAZ deficiency, we challenged Tg and NTg animals with a high-fat, dox-containing diet for 16 weeks. The TAZ kd animals gained significantly less weight (34%) compared with the NTg + dox littermates (Fig. 3*A*), exclusively because of the attenuation of fat mass (68%) (Fig. 3*B–D* and Supplementary Fig. 2*A*). The amount of TGs was also significantly reduced in both the liver (70%) and skeletal muscle (84%) of TAZ kd animals compared with the NTg + dox controls (Fig. 3*E* and *F*). While hepatic lipid-filled vacuoles were prevalent in the NTg + dox mice, they were almost completely absent in the TAZ kd group (Fig. 3*G*). This underscored the ability of TAZ deficiency to attenuate liver pathology characterized by elevated plasma ALT concentrations and hepatic macrovesicular and microvesicular steatosis (Supplementary Fig. 2*B* and *C*). The glucose intolerance, insulin resistance, and plasma hyperlipidemia that accompanied lipid accumulation in NTg + dox mice was also prevented when TAZ was knocked down (Fig. 3*H* and *I* and Supplementary Fig. 2*E–G*).

Indirect calorimetry indicated that oxygen consumption, heat production, and activity were significantly increased in TAZ kd mice fed a high-fat diet compared with NTg + dox controls (Fig. 3*J–L*). The difference in weight gain between genotypes could not be accounted for by food consumption or water intake (Supplementary Fig. 2*H* and *I*). Thus, TAZ deficiency promotes a lean phenotype as a result of hypermetabolism and hyperactivity when exposed to either a low- or a high-fat diet challenge.

Hepatic Mitochondrial Supercomplexes Are Maintained in TAZ kd Mice

It has been established that reductions in total CL and/or L_4CL levels in the heart are associated with mitochondrial respiratory chain dysfunction and the development of cardiomyopathy (4,5). Both patients with BTHS and TAZ kd mice develop a cardiomyopathy due to CL-depleted mitochondria (14,26–28). The apparent discrepancy in TAZ kd mice between reduced cardiac capacity for mitochondrial oxidative phosphorylation and the elevation in whole-body oxygen consumption compelled us to identify TAZ-deficient tissues in which mitochondrial function was preserved. One critical way that CL maintains mitochondrial function is through the assembly of electron transport chain supercomplexes (4,29). Thus we investigated the degree to which mitochondrial supercomplex formation was maintained despite TAZ deficiency in several metabolic tissues.

Initially, we confirmed previous reports that targeted TAZ kd lowered total CL and L_4CL (1,448 m/z) levels in the heart compared with littermate controls (NTg + dox;

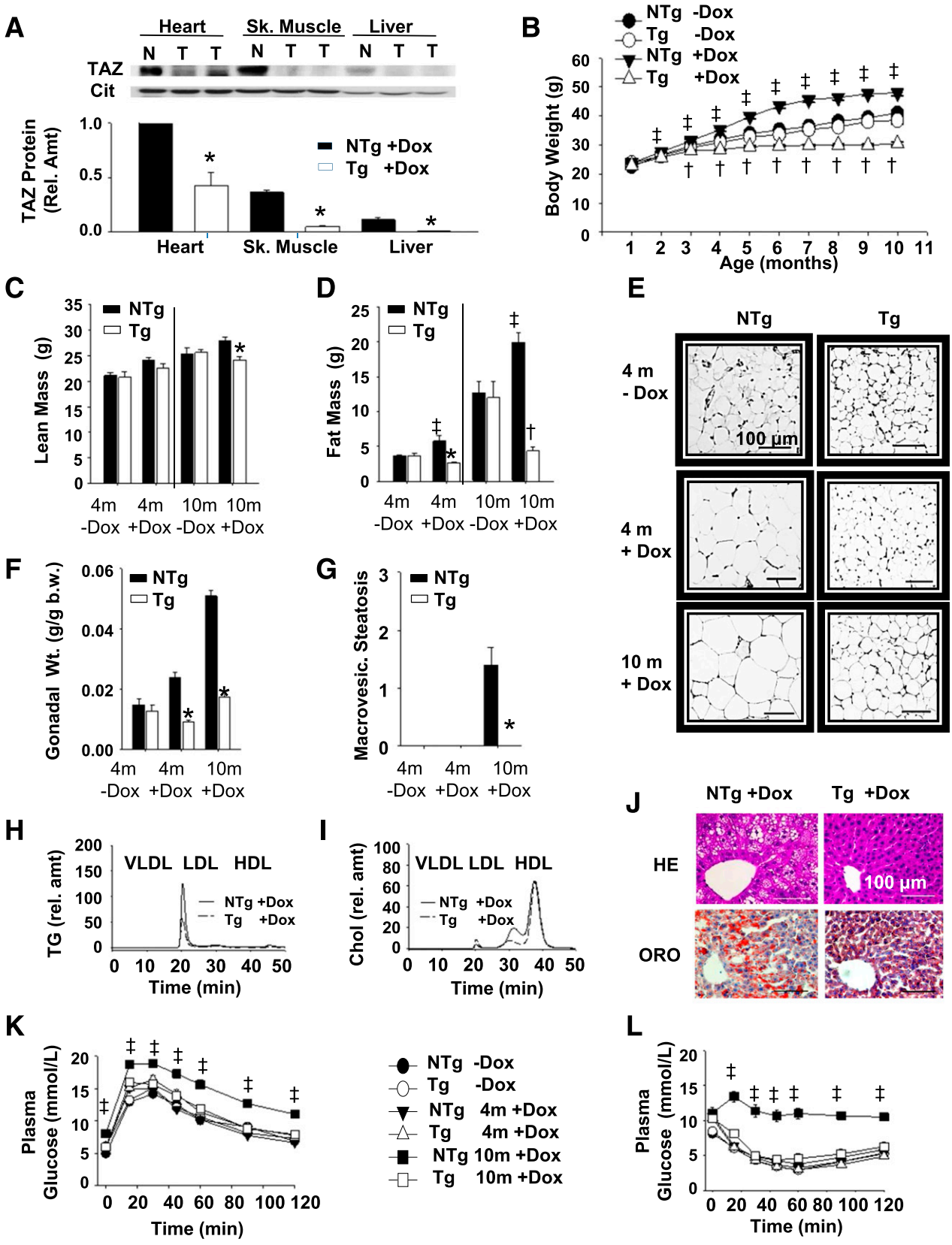

Figure 1—TAZ kd mice are protected from diet-induced obesity. *A*: Dox-inducible kd of TAZ protein in Tg (T) compared with NTg (N) mice was determined by immunoblot using isolated mitochondria (25 µg heart, 50 µg skeletal [Sk.] muscle, and 100 µg liver). Quantitation was performed with citrate synthase (Cit) as the loading control (n = 3–6). *B*: Body weights of Tg and NTg mice (n = 40). Body mass—both lean (*C*) and fat (*D*)—was measured (n = 17). *E*: Gonadal WAT stained with hematoxylin-eosin (HE; n = 5–10). *F*: Gonadal fat pad mass per body weight (b.w.) (n = 15–40). *G*: Hepatic macrovesicular (macrovesic.) steatosis was scored (n = 5–7). *H* and *I*: Plasma from fasted animals was

Table 1—Plasma, liver, and skeletal muscle parameters in TAZ-deficient mice

	TAZ-deficient mice					
Genotype	NTg	Tg	NTg	Tg	NTg	Tg
Diet	−Dox	−Dox	+Dox	+Dox	+Dox	+Dox
Age (months)	4	4	4	4	10	10
Plasma parameters						
PC (mg/dL)	72.6 ± 7.8	71.6 ± 8.1	118.6 ± 4.6	108.7 ± 3.3	218.2 ± 8.3	208.8 ± 7.6
FC (mg/dL)	11.7 ± 1.1	12.0 ± 1.3	22.0 ± 0.7	21.3 ± 0.7	32.0 ± 0.4	30.7 ± 1.3
CE (mg/dL)	79.8 ± 8.5	85 ± 9	105.2 ± 5.0	89.0 ± 2.3*	165.6 ± 4.6	145.3 ± 5.4*
TG (mg/dL)	16.4 ± 1.2	18 ± 2.5	59.5 ± 4.2	40.3 ± 5.3*	47.8 ± 4.6	34.6 ± 4.1*
NEFA (mmol/L)	0.35 ± 0.02	0.33 ± 0.02	0.39 ± 0.03	0.39 ± 0.05	0.38 ± 0.04	0.41 ± 0.04
Leptin (mg/mL)	0.51 ± 0.02	0.55 ± 0.02	1.25 ± 0.02	0.28 ± 0.01*	23.5 ± 0.02	0.18 ± 0.04*
ALT (U/L)	18.5 ± 1.0	20.0 ± 0.5	19.6 ± 1.3	15.0 ± 0.3	42.7 ± 5.6	24.3 ± 9.3*
Glucose (mmol/L)	5.0 ± 0.2	5.9 ± 0.3*	5.8 ± 0.1	6.1 ± 0.2	7.9 ± 0.3	5.7 ± 0.2*
Insulin (ng/mL)	0.59 ± 0.14	0.49 ± 0.03	0.40 ± 0.05	0.33 ± 0.05	2.17 ± 0.81	0.63 ± 0.25*
Ketones (mmol/L)	1.16 ± 0.08	1.03 ± 0.07	1.17 ± 0.06	1.03 ± 0.08	1.00 ± 0.11	1.44 ± 0.09*
TNF-α (pg/mL)	BD	BD	BD	BD	BD	BD
Adiponectin (μg/mL)	21.3 ± 2.7	20.4 ± 1.2	23.1 ± 1.1	18.4 ± 1.1*	23.5 ± 1.3	17.3 ± 0.6*
Liver parameters						
PC (nmol/mg)	75.3 ± 2.1	80.4 ± 2.2	85.8 ± 1.5	86.7 ± 3.2	66.1 ± 2.2	61.6 ± 1.2
PE (nmol/mg)	33.7 ± 1.5	40.0 ± 2.1*	42.9 ± 1.1	45.4 ± 2.0	30.7 ± 1.1	34.4 ± 1.1*
PS (nmol/mg)	4.4 ± 0.2	5.0 ± 0.3	4.8 ± 0.2	5.4 ± 0.2	5.3 ± 0.2	6.2 ± 0.3*
PI (nmol/mg)	15.5 ± 0.7	15.9 ± 0.4	15.5 ± 0.7	15.9 ± 0.4	13.5 ± 0.4	13.2 ± 0.3
FC (μg/mg)	7.6 ± 0.8	7.5 ± 0.3	7.9 ± 0.2	8.1 ± 0.1	13.2 ± 1.0	12.6 ± 0.6
CE (μg/mg)	3.9 ± 0.6	4.2 ± 0.4	3.6 ± 0.1	3.6 ± 0.1	11.7 ± 0.8	7.3 ± 1.0*
TG (μg/mg)	222.2 ± 17.8	238.6 ± 23.2	118.1 ± 12.7	92.7 ± 14.6	677.01 ± 68.1	125.6 ± 24.9*
NEFA (μg/mg)	ND	ND	ND	ND	2.3 ± 0.3	1.4 ± 0.2*
SM (μg/mg)	9.6 ± 1.0	8.2 ± 1.4	8.1 ± 0.3	8.2 ± 0.2	8.5 ± 0.6	8.6 ± 0.5
Skeletal muscle parameters						
PC (nmol/mg)	20.3 ± 2.8	31.4 ± 3.2	31.4 ± 2.2	24.1 ± 1.9	32.3 ± 2.6	25.8 ± 2.2
PE (nmol/mg)	4.9 ± 0.6	8.5 ± 0.3*	9.7 ± 1.7	7.5 ± 0.9	10.4 ± 0.8	8.9 ± 0.7
PI (nmol/mg)	3.4 ± 0.2	3.1 ± 0.3	3.3 ± 0.1	3.4 ± 0.5	3.2 ± 0.1	2.8 ± 0.1
FC (μg/mg)	1.1 ± 0.2	1.6 ± 0.2	1.3 ± 0.2	1.2 ± 0.1	1.4 ± 0.1	1.4 ± 0.1
TG (μg/mg)	31.1 ± 6.0	37.2 ± 8.8	53.2 ± 12.1	13.8 ± 4.5*	213.5 ± 16.6	28.3 ± 3.1*

Data are means ± SEMs (n = 5–17). ALT, alanine aminotransferase; BD, below detection; CE, cholesteryl ester; FC, unesterified free cholesterol; ND, not determined; NEFA, nonesterified fatty acid; PC, phosphatidylcholine; PE, phosphatidylethanolamine; PI, phosphatidylinositol; PS, phosphatidylserine; SM, sphingomyelin; TNF, tumor necrosis factor. *$P < 0.05$ compared with NTg age-matched mice fed an identical diet.

Fig. 4*A*). This was accompanied by reduced formation of cardiac supercomplexes (Fig. 4*B*) that contained complex I (Fig. 4*C* and Supplementary Fig. 3*B*) and complex IV (Fig. 4*E* and Supplementary Fig. 3*C*). The simultaneous increases in free complex I and IV indicated that the individual complexes were available but prevented from forming respirasomes in the heart of TAZ kd animals. This was additionally supported by immunoblot analysis demonstrating that total levels of complexes I and IV were the same between genotypes (Supplementary Fig. 3*A*). As expected, complex II (succinate–coenzyme Q reductase) migrated alone (Fig. 4*D*).

Mitochondria isolated from skeletal muscle and brown adipose tissue of TAZ kd mice also had significantly reduced L_4CL (1,448 m/z) (Fig. 4*F* and Supplementary Fig. 4*A*) with impaired formation of supercomplexes (Fig. 4*G*) containing complexes I (Fig. 4*H* and Supplementary Figs. 3*E* and 4*E*) and/or IV (Fig. 4*J* and Supplementary Figs. 3*F* and 4*F*). There was no significant difference between genotypes with respect to the abundance of individual complexes (Fig. 4*I* and Supplementary Figs. 3*D* and 4*D*). Interestingly, we determined that while the amount of hepatic total CL and L_4CL (1,448 m/z) were reduced in TAZ kd animals compared with the littermate controls (NTg + dox), the levels remained similar to those in animals fed a standard diet (Tg and NTg – dox; Fig. 4*K*). As a result, supercomplexes containing complex I appeared to assemble normally in the liver of TAZ kd animals (Fig. 4*L* and *M*

separated into VLDLs, LDLs, and HDLs, and TGs and total cholesterol (Chol; unesterified and esterified) were measured (n = 3–4). rel. amt, relative amount. *J*: Livers from 10-month-old animals stained with HE or Oil Red O (ORO) (n = 5–14). Glucose tolerance (*K*) and insulin tolerance (*L*) tests (n = 12–28). Data are means ± SEMs. *$P < 0.05$ compared with NTg age-matched mice fed an identical diet; †$P < 0.05$, Tg + dox compared with all other groups; ‡$P < 0.05$, NTg + dox compared with all other groups.

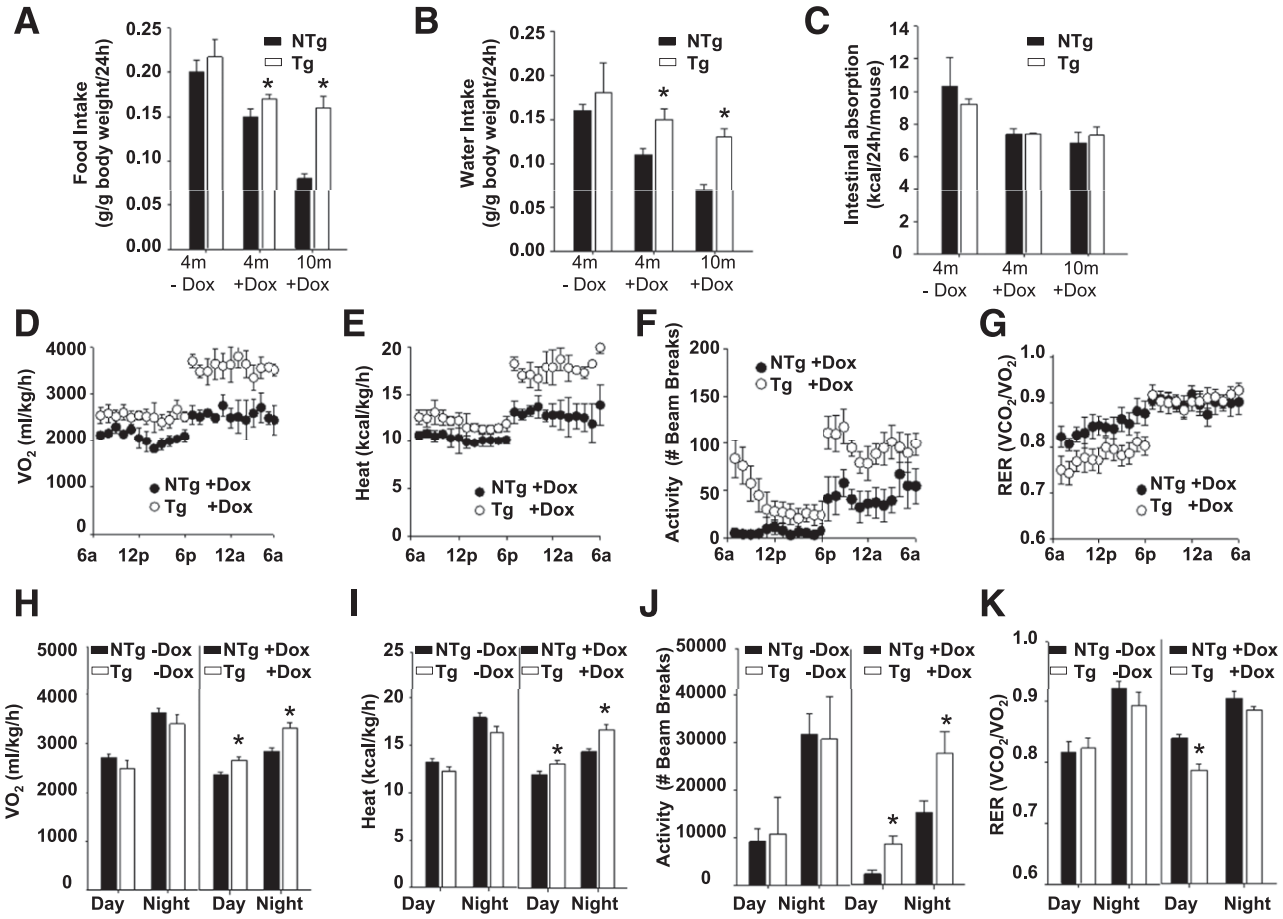

Figure 2—Hypermetabolism protects TAZ kd mice from diet-induced weight gain. Food (*A*) and water (*B*) consumption were measured in Tg and NTg mice fed a low-fat diet; values are expressed as a proportion of body weight (n = 10–20). *C*: Intestinal absorption represents the amount of calories consumed minus the amount of calories excreted in feces (n = 4–14). *D–K*: Indirect calorimetry was performed to measure oxygen consumption (Vo_2; *D* and *H*), heat production (*E* and *I*), activity (*F* and *J*), and the respiratory exchange ratio (RER; *G* and *K*). Values are the means ± SEMs of 5–14 mice per group. *$P < 0.05$ compared with NTg age-matched mice fed an identical diet.

and Supplementary Fig. 3*I*). As previously reported (30), the majority of complex IV and complex II migrated alone in the liver (Fig. 4*N* and *O* and Supplementary Fig. 3*J*). We also determined that CL levels and supercomplex formation in WAT was similar between genotypes (Supplementary Fig. 4*B*, *C*, and *G–I*). However, since uncoupling protein 1 expression was unaltered (Supplementary Fig. 1*J*) and WAT generally makes a small contribution to metabolic rate, we expected WAT to have a minor role in elevating whole-body oxygen consumption in TAZ kd mice.

A reduction in supercomplex formation is typically associated with elevated mitochondrial ROS production, primarily because of the dissociation of complex I from complex III (9). Consistent with the reduction of supercomplexes found in TAZ-deficient heart and skeletal muscle, the amount of H_2O_2 was elevated compared with littermate controls (NTg + dox; Fig. 5*A* and *B*). By contrast, ROS formation was significantly reduced in the livers of TAZ kd mice compared with NTg + dox controls, indicating improved electron flux between mitochondrial respiratory complexes (Fig. 5*C*).

Hepatic Respiratory Mitochondrial Function Is Preserved With TAZ Deficiency

We established that supercomplex formation was preserved in the livers, but not the skeletal muscle, of TAZ kd mice. Therefore we sought to determine whether mitochondrial respiratory function was maintained in a corresponding tissue-specific way by measuring the OCR. Furthermore, the use of different energy substrates provided the capability to evaluate whether the liver and/or skeletal muscle contribute to the increase in whole-body OCR that promotes the lean phenotype of TAZ kd animals.

Initially, we performed experiments using glucose as the primary energy substrate. We determined that the levels of basal and ATP-insensitive oxygen consumption (heat) were reduced in cultures of hepatocytes isolated from TAZ kd mice (Fig. 5*D* and *F*). However, a defect in mitochondrial function was not detected; the levels of hepatic ATP-sensitive (oligomycin-sensitive) oxygen consumption and maximum respiratory capacity were maintained (Fig. 5*E* and *G*). When oxygen consumption was measured from isolated intact skeletal muscle fibers, there

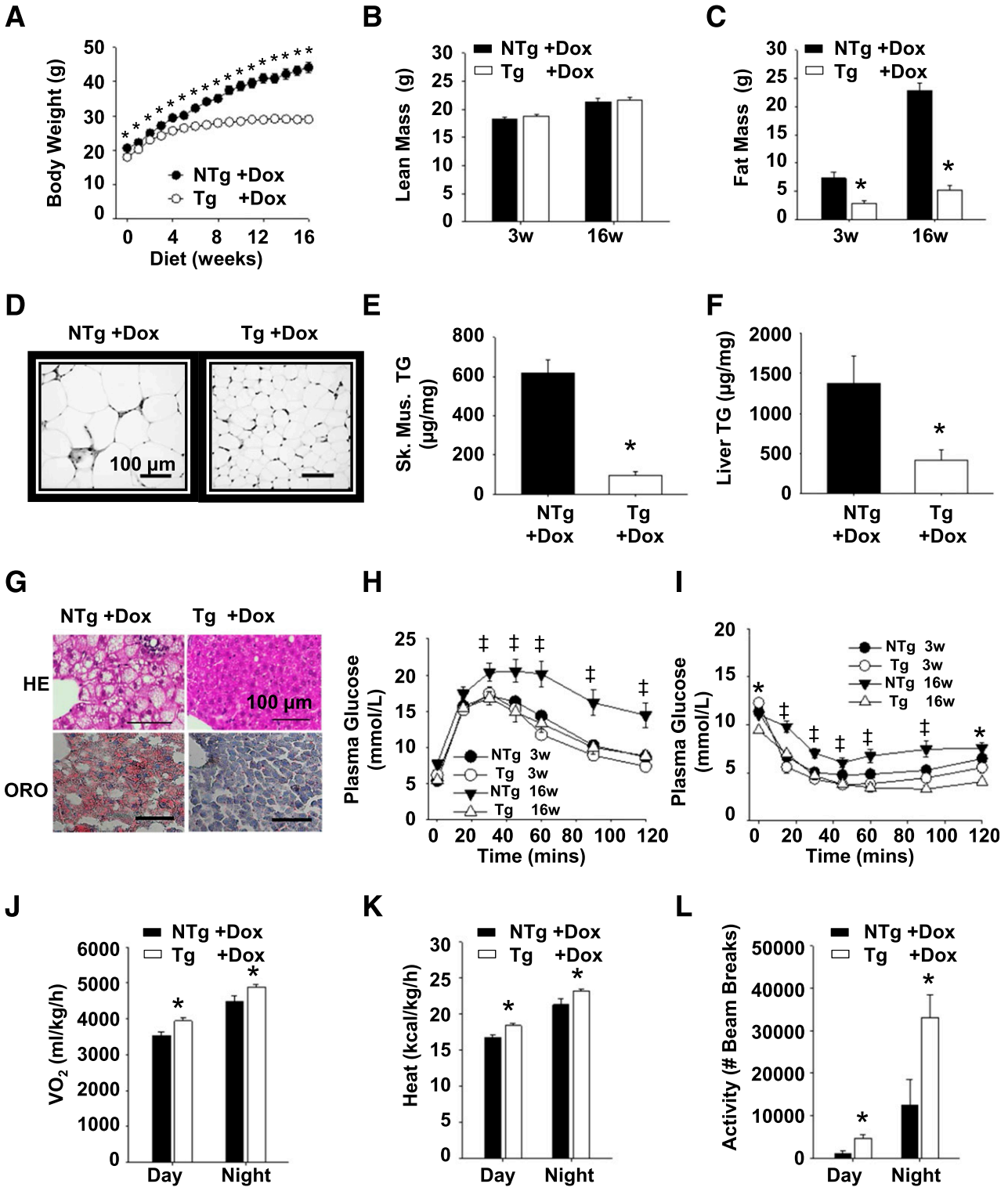

Figure 3—TAZ kd mice are protected from diet-induced obesity when fed a high-fat diet. *A*: Body weights of Tg and NTg mice fed a high-fat diet (n = 40). Lean (*B*) and fat (*C*) body masses (n = 6–13) were measured. *D*: Gonadal WAT stained with hematoxylin-eosin (HE; n = 6–10). *E* and *F*: TG quantitation in skeletal muscle (sk. musc.; soleus) (*E*) and liver (*F*) tissues (n = 8–9). *G*: Livers stained with HE or Oil Red O (ORO) (n = 3–10). Glucose tolerance (*H*) and insulin tolerance (*I*) tests (n = 14–16). *J–L*: Indirect calorimetry was performed to measure oxygen consumption (V_{O_2}; *J*), heat production (*K*), and activity (*L*) (n = 3–8). Data are expressed as means ± SEMs. *P < 0.05 compared with NTg age-matched mice fed an identical diet; ‡P < 0.05, NTg compared with all other groups.

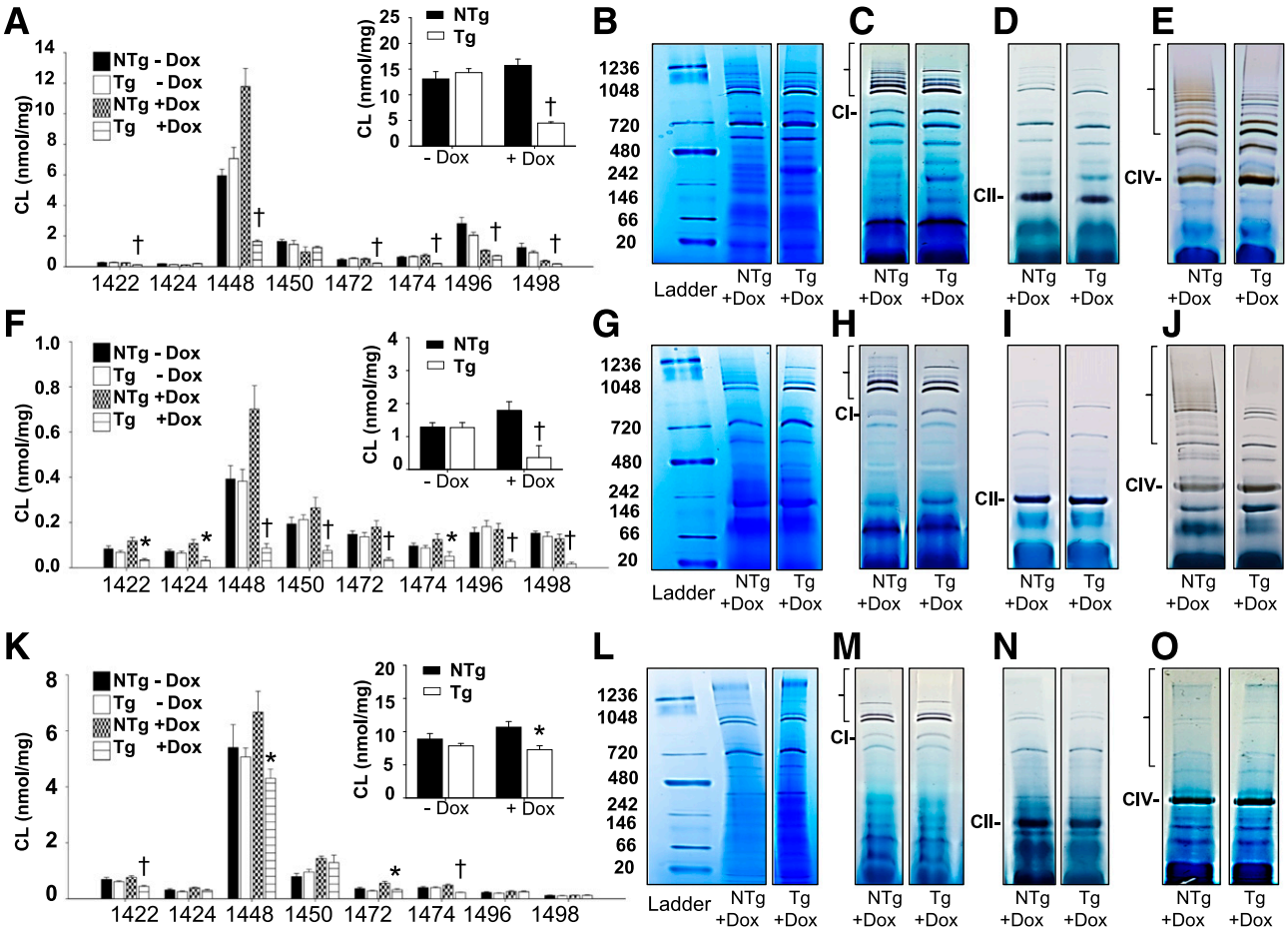

Figure 4—The quantitation of individual cardiolipin species and determination of mitochondrial supercomplex formation in various mouse tissues. Molecular species of CL were determined by mass spectrometry–mass spectrometry and arranged by mass for heart (*A*), skeletal muscle (*F*), and liver (*K*) of 4-month-old animals. Total CL content is shown in the inset for each tissue. Values are means ± SEMs (n = 5–9). Supercomplexes were separated by Blue Native PAGE for heart (*B*), skeletal muscle (*G*), and liver (*L*) before conducing in-gel activity assays for mitochondrial complexes I (*C*, *H*, and *M*), II, (*D*, *I*, and *N*), and IV (*E*, *J*, and *O*) (heart, skeletal muscle, and liver, respectively). The location of each individual complex is indicated as CI, CII, or CIV, respectively. The supercomplexes that contain the complex of interest (i.e., the active complex) are indicated with brackets at the top of each gel. The ladder size is indicated in kilodaltons on the left, and each lane is representative of 3–6 animals per group. *P < 0.05 compared with NTg age-matched mice fed an identical diet; †P < 0.05, Tg + dox compared with all other groups.

was no difference between groups (Supplementary Fig. 5*A*–*D*). These results indicated that TAZ kd tissue neither carries a defect in mitochondrial respiration nor contributes to increased oxygen consumption when glucose is the major substrate.

The absence of measureable mitochondrial respiratory dysfunction in the TAZ kd mice could reflect the capability of glucose to mask defects in oxidative phosphorylation by supporting glycolysis, as previously demonstrated for TAZ-deficient induced pluripotent stem cell–derived cardiomyocytes (31). To better assess the oxidative phosphorylation capacity and directly measure FAO, we repeated the oxygen consumption measurements in hepatocytes and muscle fibers with palmitate-BSA as the major substrate. The experiments were performed with etomoxir, which inhibits CPT1-mediated transport of FAs into the mitochondria. The difference in oxygen consumption between the absence and presence of etomoxir reveals FA-dependent metabolism. We determined that FA-dependent basal, ATP-sensitive, and ATP-insensitive (heat) oxygen consumption were elevated in the hepatocytes isolated from the TAZ kd animals compared with NTg + dox controls (Fig. 5*H*–*K*). By contrast, skeletal muscle fibers isolated from TAZ kd mice had reduced FA-dependent basal and ATP-insensitive oxygen consumption (Supplementary Fig. 5*E*–*G*). The suppression of maximum respiration from skeletal muscle fibers when FA was the major uninhibited source of energy indicated a potential defect in oxidative phosphorylation (Supplementary Fig. 5*H*). Together, these results indicated that the liver contributes to the hypermetabolism of TAZ kd animals by promoting FA-dependent oxygen consumption and heat production.

Hepatic FAO Is Elevated With TAZ Deficiency

The elevation of hepatic FAO in TAZ deficiency was confirmed when we measured increased production of acid-soluble metabolites from primary hepatocyte cultures incubated with [^{14}C]-oleate (Fig. 6*A*). In addition, fasting

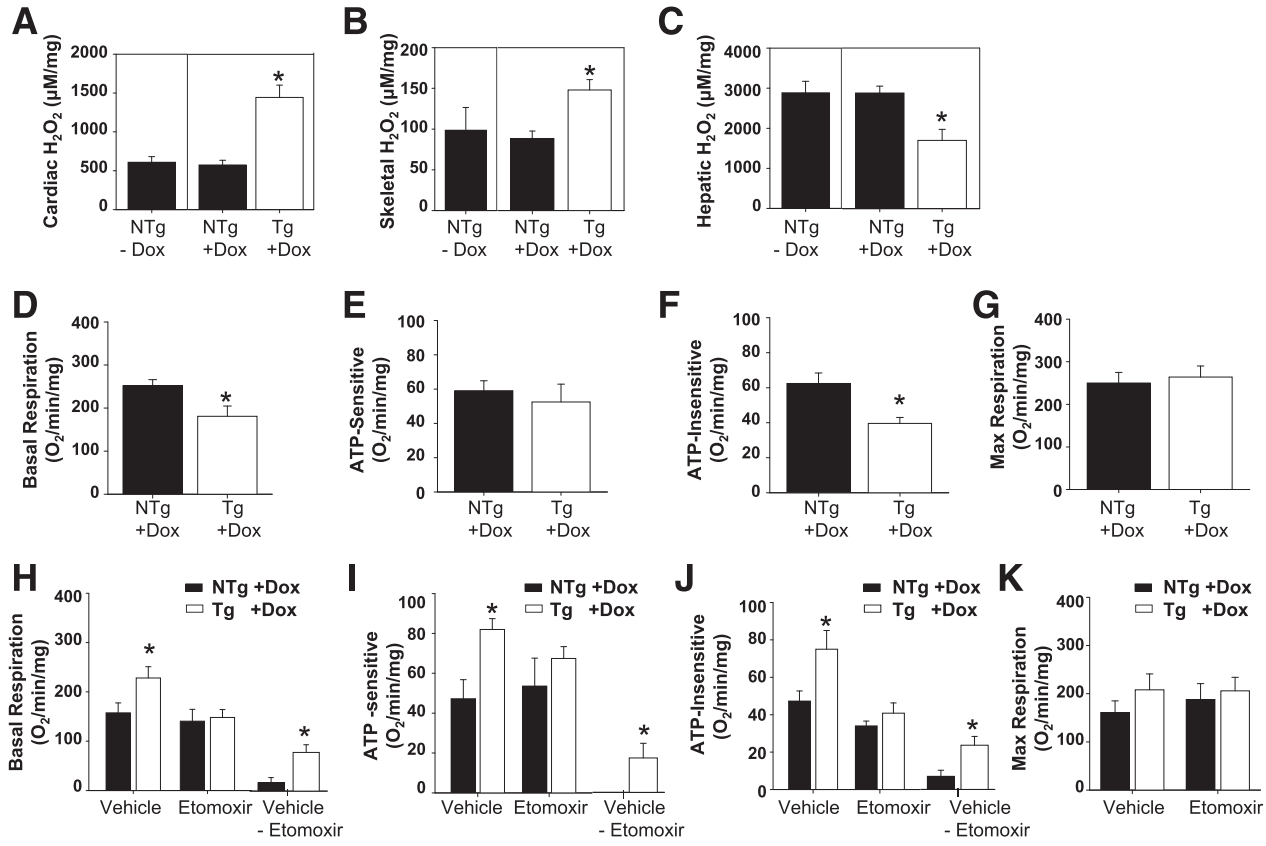

Figure 5—The assessment of mitochondrial function in TAZ kd mice. Quantification of H_2O_2 in heart (*A*), skeletal muscle (*B*), and liver (*C*) of 10-month-old Tg and NTg mice fed a diet containing dox. *D–F*: Hepatocytes were cultured in 10 mmol/L glucose, and basal respiratory (*D*), ATP-sensitive (oligomycin-sensitive; *E*), ATP-insensitive (i.e., heat; *F*), and maximum (max; FCCP; *G*) OCRs were measured; values are expressed per milligram of cellular protein (n = 4–5). *H–K*: Hepatocytes were cultured in 0.175 mmol/L palmitate-BSA in the presence of 40 μmol/L etomoxir or vehicle (water), and basal respiratory (*H*), ATP-sensitive (*I*), ATP-insensitive (*J*), and maximum (*K*) oxygen consumption were measured (n = 3–4). Values are means ± SEMs. *P < 0.05 compared with NTg age-matched mice fed an identical diet.

plasma ketone bodies, considered an accurate indicator of hepatic FAO, were elevated in the TAZ kd mice compared with NTg + dox controls (Table 1). We determined that FAO was the major way that TGs were reduced in the liver of TAZ kd mice, since FA uptake (Fig. 6*B*), TG synthesis (Fig. 6*C* and *D*), and TG secretion (Supplementary Fig. 6*A* and *B*) were similar between genotypes. Furthermore, we determined that elevated hepatic FAO was the result of increased amounts of long-chain acyl-dehydrogenase mRNA and the corresponding protein, the α subunit of mitochondrial trifunctional protein (MTPa) (Fig. 6*G–J*). The increased levels of adipose triglyceride lipase, phosphorylated hormone-sensitive lipase, plasma nonesterified FAs, and catecholamines in TAZ kd mice indicate that FA may be partly supplied by increased WAT lipolysis (Supplementary Fig. 6*H–M*).

Interestingly, we determined that CL synthesis from both [^{14}C]-oleate (Fig. 6*E*) and [^{14}C]-acetate (Fig. 6*F*) was significantly elevated in hepatocytes isolated from TAZ kd animals compared with littermate controls (NTg + dox). This was specific for CL and was not a global increase in phospholipid synthesis, as incorporation into phosphatidylcholine (PC) remained unchanged (Supplementary Fig. 6*C* and *D*). CL synthesis was promoted in TAZ deficiency by increased levels of the TAM41 protein, which catalyzes the rate-limiting step of CL synthesis and MTPa, which also encodes the CL remodeling enzyme monolysocardiolipin acyltransferase-1 (MLCLAT-1) (4) (Fig. 6*G*). MLCLAT-1 resides at the COOH terminal of MTPa and catalyzes the reacylation of CL with linoleic acid after a fatty acyl chain has been hydrolyzed by a phospholipase. The expression of MTPa was not altered in any other tissue (Supplementary Fig. 6*E–G*).

DISCUSSION

Increasing evidence suggests that mitochondrial dysfunction is central in the lipid-mediated disruption of insulin signaling during diet-induced obesity. Despite the well-established role of CL in regulating mitochondrial function, an association with metabolic syndrome had not been studied extensively. The goal of this study was to test whether reducing total CL and/or L_4CL levels resulted in mitochondrial dysfunction, leading to atypical lipid accumulation and insulin resistance. We determined that TAZ deficiency prevented diet-induced obesity after 10 months of low-fat and 16 weeks of high-fat diet feeding. The significant reduction of neutral lipid in both the liver

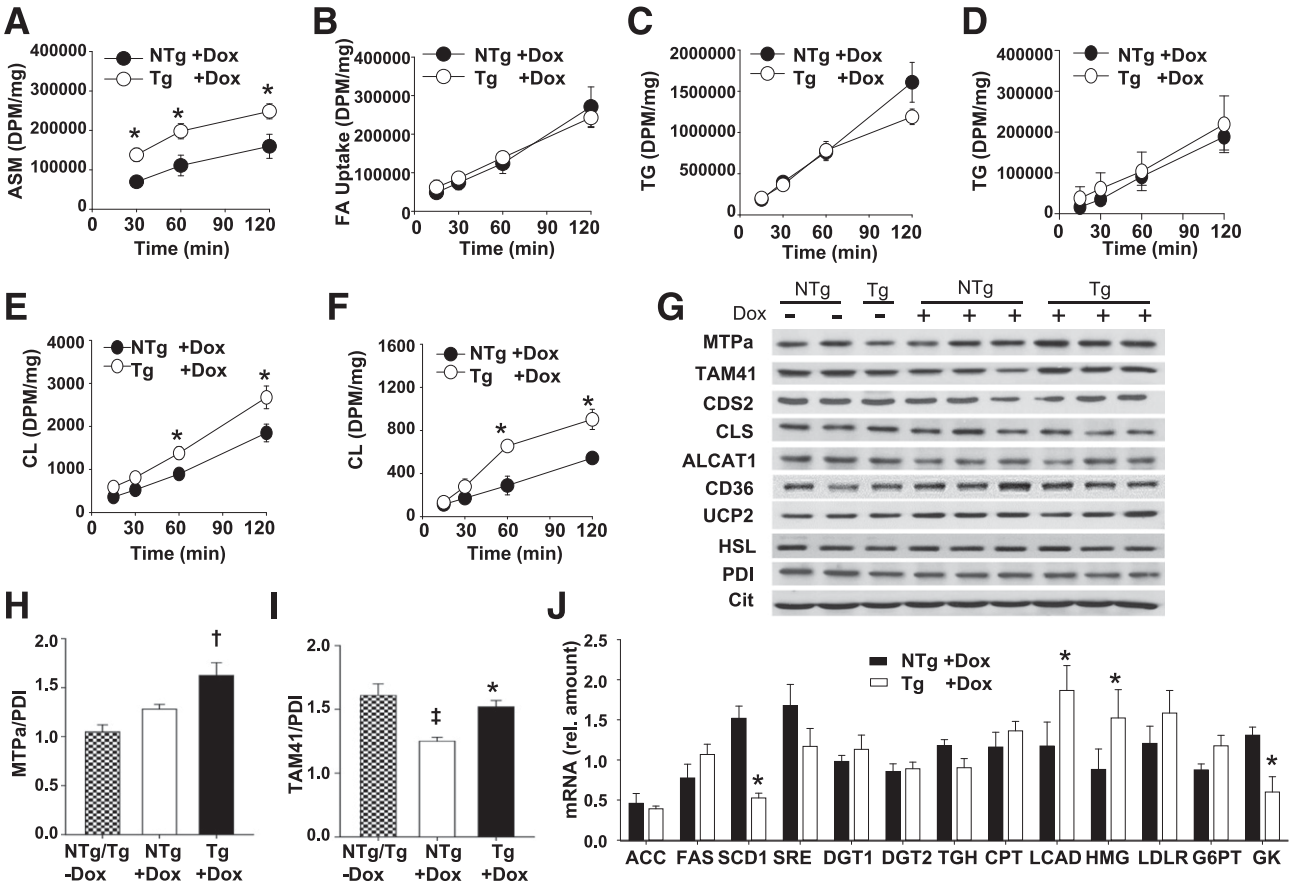

Figure 6— Increased hepatic FAO and CL synthesis in TAZ kd mice. *A–F*: Primary cultures of hepatocytes were isolated from 4-month-old NTg and Tg mice fed a diet containing dox. Cells were incubated with [^{14}C]-oleate for the durations indicated, and radiolabel was measured in the media as acid-soluble metabolites (ASMs; n = 5–6) (*A*) and in total cell lysate (n = 5–6) (*B*). Hepatocytes were incubated with [^{14}C]-oleate (*C* and *E*) or [^{14}C] acetate (*D* and *F*) for the durations indicated, and the incorporation of radiolabel into TG and CL was measured (n = 4–6). *G*: Immunoblot of MTPa, TAM41, ALCAT1, cardiolipin synthase (CLS), uncoupling protein 2 (UCP2), CD36, hormone-sensitive lipase (HSL), and loading control (protein disulfide isomerase [PDI]) in liver lysates and CDP-diacylglycerol synthase 2 (CDS2) and a loading control (citrate synthase) in isolated liver mitochondria (20 μg protein). *H* and *I*: Quantitation of immunoblots by densitometry with normalization against PDI (n = 3–6). *J*: The mRNA levels of the indicated genes measured in the liver by quantitative PCR. DPM, disintegrations per minute; rel., relative. All data are means ± SEMs (n = 3–7). *P < 0.05 compared with NTg age-matched mice fed an identical diet; †P < 0.05, Tg +dox compared to all other groups; ‡P < 0.05, NTg +dox compared to all other groups.

and skeletal muscle correspondingly accompanied the prevention of insulin resistance in the TAZ kd animals.

Using indirect calorimetry, we determined that the lean phenotype of TAZ kd mice was caused by hypermetabolism as a result of increased energy consumption, elevated heat production, and activity. The increase in hepatic mitochondrial oxygen consumption and heat production mirrored whole-body data when FA was the oxidative substrate. This result indicated a central role for hepatic FAO in providing protection against diet-induced obesity in TAZ kd mice (Fig. 7). Curiously, the liver supported increased FAO, despite evidence that TAZ deficiency in the heart is linked to reduced mitochondrial function and impaired FAO (26,28,31). We attributed this discrepancy to the ability of the liver to maintain normal CL levels. An increase in the expression of CL synthetic/remodeling enzymes (MLCLAT-1 and TAM41) in the liver compensated for the reduction in TAZ expression. We found significant increases in hepatic CL biosynthesis from both acetate- and oleate-radiolabeled precursors in the TAZ kd animals. This increase in biosynthesis achieved total hepatic CL and L_4CL levels (80–90%) similar to those of mice fed a standard rodent diet (Tg and NTg – dox). The small but significant reduction (~30%) of CL and L_4CL in the livers of TAZ kd mice compared with the littermate controls (NTg + dox) did not have any detectable negative physiological effect on mitochondrial function: supercomplex stability was preserved, ROS formation reduced, and mitochondrial oxidative metabolism maintained. In previous studies mitochondrial dysfunction occurred in the liver when CL and/or L_4CL levels were reduced by >35% (32,33). Similar reductions in CL have also accompanied mitochondrial dysfunction in the myocardium (6,8). In our recent study using heterozygous *Mtpa* knockout mice, small reductions (~25–30%) in CL and L_4CL in the heart and liver were found to have no effect on supercomplexes in

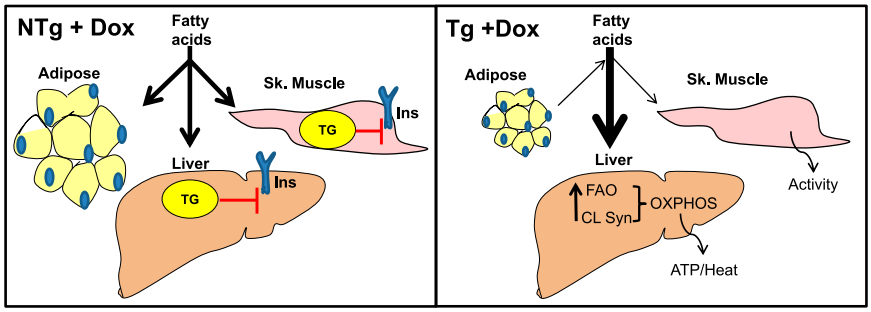

Figure 7—Schematic summary. In NTg + dox control animals, circulating FAs are taken up by the liver and adipose and skeletal (Sk.) muscle and are stored as TGs. The resulting accumulation of lipids has lipotoxic effects on insulin signaling (Ins). In TAZ deficiency (Tg + dox), increased CL synthesis (CL Syn) maintains the total CL levels necessary for hepatic mitochondrial supercomplex formation. These supercomplexes provide efficient mitochondrial oxidative phosphorylation (OXPHOS) to support the generation of heat and ATP from the increase in FAO. Overall excess FAs are directed toward hepatic FAO and away from TG stores in the liver and adipose and skeletal muscle, resulting in normal whole-body insulin sensitivity.

either tissue (34). Thus more severe reductions in total CL and/or L_4CL are required to impair mitochondrial function, regardless of tissue type.

FAO in the liver is beneficial in the context of overfeeding. FAO directs excess FAs away from TG synthesis and the subsequent generation of various lipotoxic molecules that promote insulin resistance (35). The results from the current study also support this theory, since increased hepatic FAO correlated with reduced hepatic TG levels and improved insulin sensitivity in the TAZ kd mice. For skeletal muscle, it is proposed that the mismatch between high FA supply and low energy demand promotes increased but incomplete mitochondrial FAO, leading to the generation of lipotoxic by-products (35). Thus the reduction in skeletal FAO observed in the TAZ kd mice may be providing some protection against developing whole-body insulin resistance. The significantly higher rates of locomotor activity in the TAZ kd mice could also increase the demand for muscular energy and alleviate mismatch with FA supply. It is, however, difficult to align the mitochondrial dysfunction observed in the skeletal muscle of TAZ kd mice with a beneficial effect. An alternative notion is that the liver may be shielding the skeletal muscle from exposure to excess lipid supply by acting as a "sink" for FA utilization (Fig. 7). This would potentially protect the skeletal muscle from lipotoxic accumulation, regardless of mitochondrial dysfunction. Previous studies have shown that a targeted approach to increase FAO in the liver of ob/ob and db/db mice fed a high-fat diet reversed and/or prevented diet-induced obesity, hepatic steatosis, whole-body insulin resistance, and the accumulation of lipotoxic metabolites in the skeletal muscle (36–38).

Our data indicate that the combined increase in hepatic CL biosynthesis and FAO prevent lipotoxic events in the TAZ kd mice. Coordination of these processes is justifiable based on the subcellular localization of the β-oxidation cycle and the core CL biosynthetic machinery to the inner mitochondrial matrix. We previously established a direct link between CL synthesis and mitochondrial β-oxidation (34,39). MLCLAT-1 activity was increased when MTPa was expressed in cell culture (39) and reduced in mice heterozygous for MTPa (34). Because metabolic derangement is closely associated with loss of CL, a coordinated increase in FAO and CL remodeling may be an attempt by hepatocytes to maintain normal mitochondrial energy production. Hepatic CL and/or L_4CL content was increased in several animal models of diabetes and nonalcoholic fatty liver disease, presumably as a metabolic adaptation, since mitochondrial complex activity was maintained (13,40,41). Furthermore, it was established that the coordinated increase in MTPa expression and CL biosynthesis was the molecular mechanism responsible for enhanced mitochondrial complex activity and FAO and reduced ROS production in mice lacking the CL remodeling enzyme ALCAT1 (11).

In conclusion, we showed that TAZ deficiency prevents the development of diet-induced obesity, hepatic steatosis, hyperlipidemia, and insulin resistance. We determined that the beneficial effect of TAZ deficiency is directly linked to the preservation of hepatic CL levels, mitochondrial supercomplexes, and respiratory function. Finally, we identified elevated hepatic FAO and CL biosynthesis as the responsible molecular mechanisms. We suggest that altering hepatic CL remodeling serves as a novel therapeutic option for patients at risk for type 2 diabetes.

Acknowledgments. The authors thank Dr. Tooru Mizuno, Department of Physiology, University of Manitoba, for the use of indirect calorimetry equipment.
Funding. This work was supported in part by grants from the Heart and Stoke Foundation of Canada, Canadian Institutes for Health Research (CIHR), the Barth Syndrome Foundation (to G.M.H.), the National Institutes of Health (grant R01HL108882 to S.M.C.), and trainees awards from the CIHR Integrated and Mentored Pulmonary and Cardiovascular Training program (to L.K.C.) and Research Manitoba/Children's Hospital Research Institute of Manitoba (to E.M.M.). G.M.H. is the Canada Research Chair in Molecular Cardiolipin Metabolism.
Duality of Interest. No potential conflicts of interest relevant to this article were reported.
Author Contributions. L.K.C., E.M.M., M.V., G.C.S., S.M.C., L.D.-C., and J.K. performed experiments. L.K.C. and G.M.H. conceptually developed the study and wrote and edited the manuscript. G.M.H. is the guarantor of this work and,

as such, had full access to all the data in the study and takes responsibility for the integrity of the data and the accuracy of the data analysis.

References

1. Kelly T, Yang W, Chen CS, Reynolds K, He J. Global burden of obesity in 2005 and projections to 2030. Int J Obes 2008;32:1431–1437
2. Sellayah D, Cagampang FR, Cox RD. On the evolutionary origins of obesity: a new hypothesis. Endocrinology 2014;155:1573–1588
3. Kim JA, Wei Y, Sowers JR. Role of mitochondrial dysfunction in insulin resistance. Circ Res 2008;102:401–414
4. Mejia EM, Cole LK, Hatch GM. Cardiolipin metabolism and the role it plays in heart failure and mitochondrial supercomplex formation. Cardiovasc Hematol Disord Drug Targets 2014;14:98–106
5. Raja V, Greenberg ML. The functions of cardiolipin in cellular metabolism-potential modifiers of the Barth syndrome phenotype. Chem Phys Lipids 2014; 179:49–56
6. Mulligan CM, Sparagna GC, Le CH, et al. Dietary linoleate preserves cardiolipin and attenuates mitochondrial dysfunction in the failing rat heart. Cardiovasc Res 2012;94:460–468
7. Heerdt PM, Schlame M, Jehle R, Barbone A, Burkhoff D, Blanck TJ. Disease-specific remodeling of cardiac mitochondria after a left ventricular assist device. Ann Thorac Surg 2002;73:1216–1221
8. Saini-Chohan HK, Dakshinamurti S, Taylor WA, et al. Persistent pulmonary hypertension results in reduced tetralinoleoyl-cardiolipin and mitochondrial complex II + III during the development of right ventricular hypertrophy in the neonatal pig heart. Am J Physiol Heart Circ Physiol 2011;301:H1415–H1424
9. Maranzana E, Barbero G, Falasca AI, Lenaz G, Genova ML. Mitochondrial respiratory supercomplex association limits production of reactive oxygen species from complex I. Antioxid Redox Signal 2013;19:1469–1480
10. Dudek J, Cheng IF, Balleininger M, et al. Cardiolipin deficiency affects respiratory chain function and organization in an induced pluripotent stem cell model of Barth syndrome. Stem Cell Res (Amst) 2013;11:806–819
11. Li J, Romestaing C, Han X, et al. Cardiolipin remodeling by ALCAT1 links oxidative stress and mitochondrial dysfunction to obesity. Cell Metab 2010;12: 154–165
12. Han X, Yang J, Yang K, Zhao Z, Abendschein DR, Gross RW. Alterations in myocardial cardiolipin content and composition occur at the very earliest stages of diabetes: a shotgun lipidomics study. Biochemistry 2007;46:6417–6428
13. Ferreira FM, Seiça R, Oliveira PJ, et al. Diabetes induces metabolic adaptations in rat liver mitochondria: role of coenzyme Q and cardiolipin contents. Biochim Biophys Acta 2003;1639:113–120
14. Acehan D, Vaz F, Houtkooper RH, et al. Cardiac and skeletal muscle defects in a mouse model of human Barth syndrome. J Biol Chem 2011;286:899–908
15. Lu YW, Galbraith L, Herndon JD, et al. Defining functional classes of Barth syndrome mutation in humans. Hum Mol Genet 2016;25:1754–1770
16. Klaunig JE, Goldblatt PJ, Hinton DE, Lipsky MM, Chacko J, Trump BF. Mouse liver cell culture. I. Hepatocyte isolation. In Vitro 1981;17:913–925
17. Folch J, Lees M, Sloane Stanley GH. A simple method for the isolation and purification of total lipides from animal tissues. J Biol Chem 1957;226:497–509
18. Cole LK, Jacobs RL, Vance DE. Tamoxifen induces triacylglycerol accumulation in the mouse liver by activation of fatty acid synthesis. Hepatology 2010; 52:1258–1265
19. Graeve M, Janssen D. Improved separation and quantification of neutral and polar lipid classes by HPLC-ELSD using a monolithic silica phase: application to exceptional marine lipids. J Chromatogr B Analyt Technol Biomed Life Sci 2009; 877:1815–1819
20. Rouser G, Siakotos AN, Fleischer S. Quantitative analysis of phospholipids by thin-layer chromatography and phosphorus analysis of spots. Lipids 1966;1:85–86
21. Sparagna GC, Johnson CA, McCune SA, Moore RL, Murphy RC. Quantitation of cardiolipin molecular species in spontaneously hypertensive heart failure rats using electrospray ionization mass spectrometry. J Lipid Res 2005;46:1196–1204
22. Ordovas JM, Osgood D. Preparative isolation of plasma lipoproteins using fast protein liquid chromatography (FPLC). Methods Mol Biol 1998;110:105–111
23. Millar JS, Cromley DA, McCoy MG, Rader DJ, Billheimer JT. Determining hepatic triglyceride production in mice: comparison of poloxamer 407 with Triton WR-1339. J Lipid Res 2005;46:2023–2028
24. Kleiner DE, Brunt EM, Van Natta M, et al.; Nonalcoholic Steatohepatitis Clinical Research Network. Design and validation of a histological scoring system for nonalcoholic fatty liver disease. Hepatology 2005;41:1313–1321
25. Bailey LC, Forrest CB, Zhang P, Richards TM, Livshits A, DeRusso PA. Association of antibiotics in infancy with early childhood obesity. JAMA Pediatr 2014;168:1063–1069
26. Powers C, Huang Y, Strauss A, Khuchua Z. Diminished exercise capacity and mitochondrial bc1 complex deficiency in tafazzin-knockdown mice. Front Physiol 2013;4:74
27. Phoon CK, Acehan D, Schlame M, et al. Tafazzin knockdown in mice leads to a developmental cardiomyopathy with early diastolic dysfunction preceding myocardial noncompaction. J Am Heart Assoc 2012;1:e000455
28. Kiebish MA, Yang K, Liu X, et al. Dysfunctional cardiac mitochondrial bioenergetic, lipidomic, and signaling in a murine model of Barth syndrome. J Lipid Res 2013;54:1312–1325
29. Pfeiffer K, Gohil V, Stuart RA, et al. Cardiolipin stabilizes respiratory chain supercomplexes. J Biol Chem 2003;278:52873–52880
30. Acín-Pérez R, Fernández-Silva P, Peleato ML, Pérez-Martos A, Enriquez JA. Respiratory active mitochondrial supercomplexes. Mol Cell 2008;32:529–539
31. Wang G, McCain ML, Yang L, et al. Modeling the mitochondrial cardiomyopathy of Barth syndrome with induced pluripotent stem cell and heart-on-chip technologies. Nat Med 2014;20:616–623
32. Petrosillo G, Portincasa P, Grattagliano I,et al. Mitochondrial dysfunction in rat with nonalcoholic fatty liver involvement of complex I, reactive oxygen species and cardiolipin. Biochim Biophys Acta 2007;1767:1260–1267
33. Hagen TM, Ingersoll RT, Wehr CM, et al. Acetyl-L-carnitine fed to old rats partially restores mitochondrial function and ambulatory activity. Proc Natl Acad Sci U S A 1998;95:9562–9566
34. Mejia EM, Ibdah JA, Sparagna GC, Hatch GM. Differential reduction in cardiac and liver monolysocardiolipin acyltransferase-1 and reduction in tetralinoleoyl-cardiolipin in the alpha subunit of trifunctional protein heterozygous knockout mice. Biochem J 2015;471:123–129
35. Muoio DM, Newgard CB. Mechanisms of disease: molecular and metabolic mechanisms of insulin resistance and beta-cell failure in type 2 diabetes. Nat Rev Mol Cell Biol 2008;9:193–205
36. An J, Muoio DM, Shiota M, et al. Hepatic expression of malonyl-CoA decarboxylase reverses muscle, liver and whole-animal insulin resistance. Nat Med 2004;10:268–274
37. Monsénégo J, Mansouri A, Akkaoui M, et al. Enhancing liver mitochondrial fatty acid oxidation capacity in obese mice improves insulin sensitivity independently of hepatic steatosis. J Hepatol 2012;56:632–639
38. Orellana-Gavaldà JM, Herrero L, Malandrino MI, et al. Molecular therapy for obesity and diabetes based on a long-term increase in hepatic fatty-acid oxidation. Hepatology 2011;53:821–832
39. Taylor WA, Mejia EM, Mitchell RW, Choy PC, Sparagna GC, Hatch GM. Human trifunctional protein alpha links cardiolipin remodeling to beta-oxidation. PLoS One 2012;7:e48628
40. Aoun M, Fouret G, Michel F, et al. Dietary fatty acids modulate liver mitochondrial cardiolipin content and its fatty acid composition in rats with non alcoholic fatty liver disease. J Bioenerg Biomembr 2012;44:439–452
41. Simões C, Domingues P, Ferreira R, et al. Remodeling of liver phospholipidomic profile in streptozotocin-induced diabetic rats. Arch Biochem Biophys 2013;538:95–102